2024 International Conference on Simulation of Semiconductor Processes and Devices (SISPAD) | 979-8-3315-1635-2/24/$31.00 ©2024 IEEE | DOI: 10.1109/SISPAD62626.2024.10733315

Atomistic Simulations of the Impact of Rotational Twin Planes Defects on the Optical Properties of InP Systems

Christian Dam Vedel and Vihar Georgiev, *Senior Member, IEEE*

***Abstract*— This paper aims to investigate the correlation between defects and device performance of III-V materials. More specifically the material under investigation here is InP. To establish such correlation between defects and material optical absorption we have performed numerical experiments. All our simulations are based on the first principle (atomistic) methodology, and specifically on the Density Functional Theory (DFT) method. By executing numerical experiments based on the DFT simulations, we have evaluated the impact of specific types of defects, called rotational twin planes (RTPs), on material properties, such as photo-absorption. We have also investigated how the RTP defects are distributed into two types of crystallographic orientations, diamond-like Zincblende (ZB) phase and meta-stable lonsdaleite-like Wurtzite (WZ) phase. Moreover, we have established a link between the material properties and the underlying electronic structure. Our work shows that the number and the orientation of RTPs in InP material have almost no impact on the absorption properties. Indeed, this could be beneficial information from a device fabrication perspective because the presence or absence of such RTP defects will have almost no impact on the device performance.**

***Index Terms*— material simulations, numerical simulations, atomistic modeling, III-V materials, InP material, defects.**

I. Introduction

Integration of III–V materials into the silicon platform is widely used to fabricate different types of devices, such as optical detectors and avalanche photodiodes [1] [2], and even novel devices, such as topological lasers [3] [4] or superconductive qubit couplers [5]. Moreover, the integration of III-V materials with Si usually yields many fabrications challenges. One such problem is the formation of defects in the III-V material. The presence of crystal defects is mainly due to a lattice mismatch between the silicon substrate and the III–V materials. To minimise the formation of such defects and to mitigate their impact on the device performance, a significant amount of research has been performed to investigate how to avoid the formation of defects, such as threading dislocations [6] [7] or rotational twin planes (RTPs) [8] [9] [10]. One possible technology that can imitate the formation of defects in III-V materials is the so-called Template Assisted Selective Epitaxy (TASE), which offers an attractive monolithic integration route for III-V semiconductors on Si, benefitting from reduced defect density devices [11].

This project has received funding from the European Union's Horizon 2020 research and innovation program under Grant Agreement No. 860095 MSCAITN-EID DESIGN-EID.

Dr Christian Dam Vedel and Prof. Vihar Georgiev are with the DeepNano Group at the James Watt School of Engineering, University of Glasgow, G12 8QQ, UK. Corresponding author email: vihar.georgiev@glasgow.ac.uk

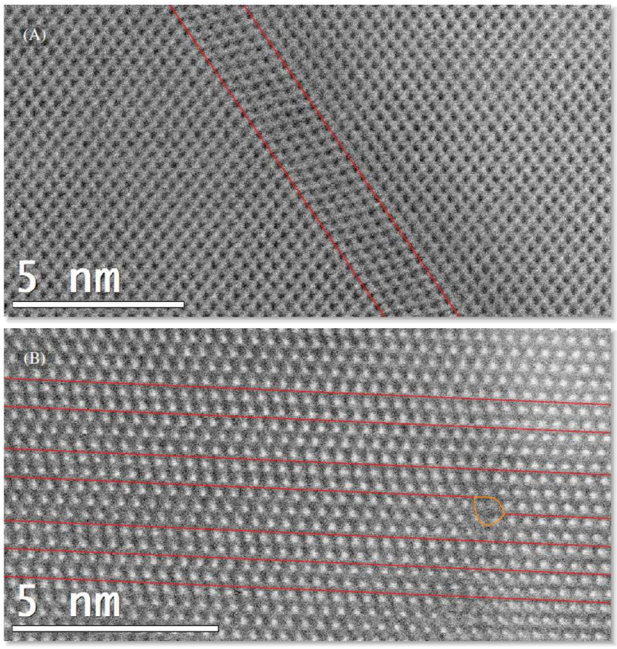

Fig. 1. High-resolution scanning transmission electron microscopy images of bulk InP viewed from the ⟨1 1 0⟩-direction, which allows visualisation of the stacking sequence along the ⟨1 1 1⟩-direction. Rotational Twin Planes (RTPs) are indicated with red lines and the line defect by an orange oval. (A) A near-perfect crystalline zincblende (ZB) lattice with only a few RTPs. (B) A highly polytypic mixed zincblende (ZB) and wurtzite (WZ) lattice with many RTPs/stacking faults and a line defect going into the image.

However, if the defects can be controlled, they can be beneficial for the device performance. Or if they are not beneficial, they do not need to be detrimental by enhancing key figures of merit, such as drive current and optical absorption. Hence, in this paper, we would like to answer the question if a specific type of defects, such as RTPs, has any impact of the photo absorption in InP materials and devices made of it.

II. Methodology

For our simulations we used the first-principles method density functional theory (DFT), as implemented in the U2022.12 version of the state-of-the-art simulation software suite QUANTUMATK by Synopsys [12]. Atoms are treated explicitly by their linear combination of atomic orbitals

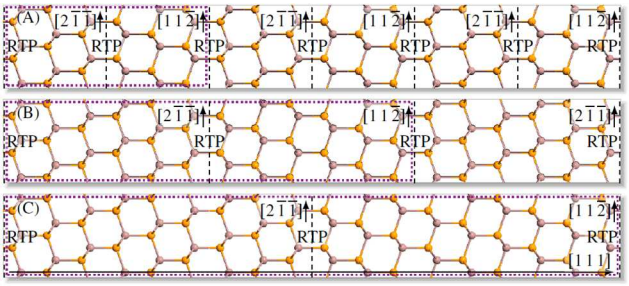

Fig. 2. Different systems of Rotational Twin Plane (RTPs) of InP simulated in this work. The purple dotted boxes indicate the utilised simulation unit cells. RTPs are indicated by dashed lines and the simulation domain of all structure has the same length for fair comparison. (A) 1 RTP every 3 layers of Zincblende (ZB). (B) 1 RTP every 6 layers of Zincblende. (C) 1 RTP every 9 layers of Zincblende.

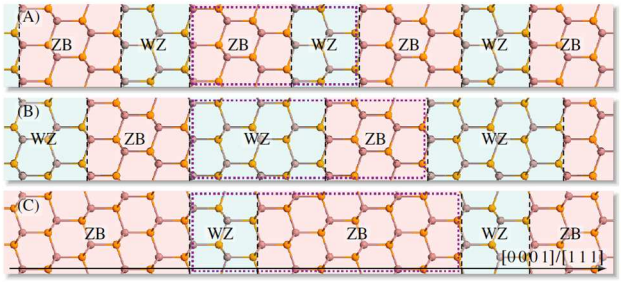

Fig. 3. Different phase mixing InP systems simulated in this paper. The purple dotted boxes indicate the utilised simulation unit cells. RTPs are indicated by dashed lines and the simulation domain of all structure has the same length for fair comparison. For illustration purpose, the Zincblende (ZB) and the Wurtzite (WZ) segments coloration terminates in the middle of the layers to indicate that these layers are shared between both segments. (A) 2 WZ layers every 3 ZB. (B) 4 WZ layers every 3 layers of ZB. (C) 2 WZ layers every 6 layers of ZB.

(LCAO) basis sets and the corresponding pseudopotential. We used the "medium" version of the PSEUDODOJO basis set [13], together with a Brillouin zone sampling density of 6 Å and a density mesh cutoff of 105 Ha. For the occupation smearing function we used a Fermi-Dirac distribution at 300 K. All investigated systems were relaxed, until the forces between the atoms were smaller than 0.05 eV/Å and the stress was lower than 0.1 GPa. For the exchange correlation functional, we used the generalised gradient approximation (GGA) functional developed by Perdew, Burke, and Ernzerhof (PBE) [14]. Phonon dispersions were calculated with finite differences using the Wigner-Seitz method to reduce the computation time.

III. Results and Discussions

InP is a direct band gap III-V semiconductor that usually crystallises in the diamondlike Zincblende (ZB) phase. Yet in recent years, it has also become possible to stabilise moderately-sized bulks of InP in its meta-stable lonsdaleite-like Wurtzite (WZ) phase [15]. Zincblende, like diamond, consists of two interwoven Face-Centered Cubic (FFC) structures, which can be described by a single FCC, and as such has a minimal unit cell consisting of two atoms. ZB differentiates from the diamond structure by having the two FCC lattices occupied solely by elements of opposite polarity,

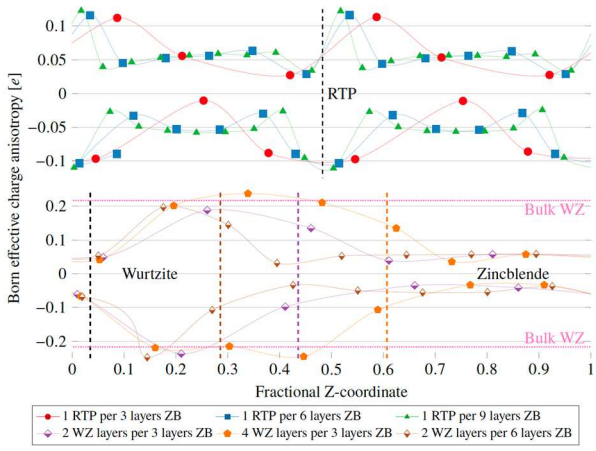

Fig. 4. Born effective charge anisotropies of RTP and phase mixing systems plotted along the fractional z-coordinate, which is the axis of the stacking sequence. Lines between points are only added for visual guidance and reflect no physical effects. Large absolute anisotropies indicate larger Born effective charges along the [0 0 0 1]-direction as compared to the [1 0 1 0]-direction. For the RTP systems, the systems are shifted so that their RTPs are matched to coincide, and their location is marked by the dashed line. For the phase mixing systems, the systems are shifted so that one interface is matched across the systems, marked by the dashed black line. The other interfaces are marked by dashed lines in their systems respective colours. The anisotropy of bulk Wurtzite is also plotted by the dotted pink line for reference.

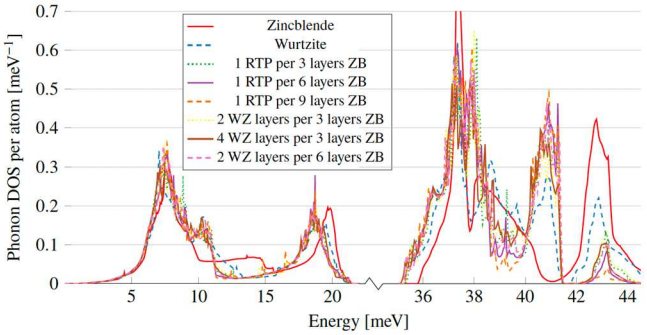

Fig. 5. Phonon DOS per atom of InP polytypic systems. The non-analytic contribution is included in the dynamical matrix, which was calculated with the Wigner-Seitz method using 5x5x3 repetition super cells.

which are indium and phosphor, in the case of InP. In the same way that ZB is similar to the diamond structure, WZ is similar to the lonsdaleite structure, i.e. hexagonal diamond, with the elemental species of opposite polarity occupying separate sub-lattices. ZB and WZ systems have direct band structures with a band gap of 1.34 eV and 1.41eV, respectively.

Fig. 1 shows two examples of grown InP, inspected with High-Resolution Scanning Transmission Electron Microscopy (HRSTEM) from the ⟨1 1 0⟩-direction. This direction of view allows visualisation of the stacking sequence along the ⟨1 1 1⟩-direction, which is the easiest method to visualise RTPs. Fig. 1 (A) shows a near-pristine sparsely twinned Zincblende (ZB) lattice. Fig. 1(B) shows a densely twinned, highly intermixed zincblende/wurtzite (WZ) lattice. A line defect

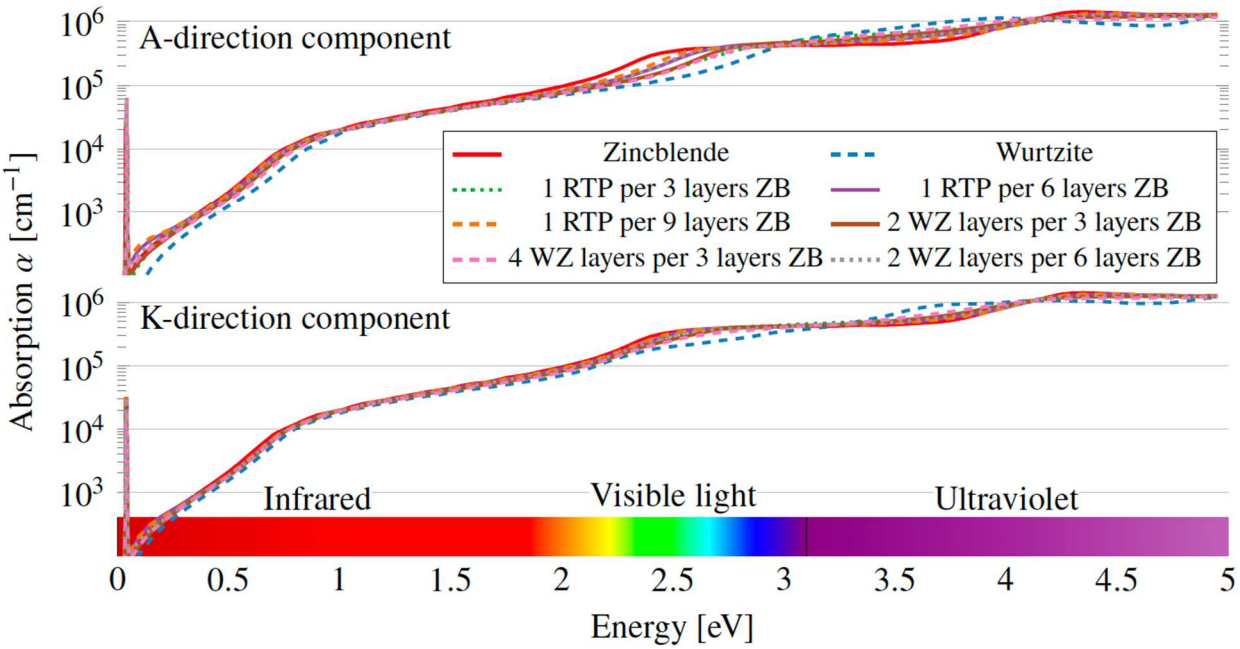

Fig. 6. Photo-absorption of polytypic InP systems along both the A- and K-directions. The sharp peaks at low energies are due to low broadenings of the ionic contributions to the dielectric functions used to calculate the absorption coefficients. The electromagnetic spectrum is illustrated for easier comprehension of the energy to wavelength relation.

appearing to be oriented along the ⟨1 1 0⟩-direction is shown to distort the crystalline lattice. The formation of RTPs is random, and they can occur in high or low densities throughout the material.

To simulate the variability shown in Fig. 1, in Fig. 2 we present the simulation unit cell of three types of InP materials with different combinations and numbers of RTPs. The resulting structure, viewed from the ⟨1 1 0⟩-directions, such as in Fig. 1, appears as a mirror image in the defect plane with its atomic species swapped. This is why the defect is called a twin. RTPs are often also called stacking faults since they are an interruption of the regular ABC-stacking sequence of ZB along the ⟨1 1 1⟩-directions. The two layers on either side of the defect plane, the last unrotated layer and the first rotated layer, together form a 2-layer WZ segment. Since both layers can either be attributed to this WZ segment or to their own respective ZB lattices, this will not be considered a true WZ segment in this work. For a similar reason, the highest density of RTPs possible in a system is one RTP every three layers of ZB in order for the ZB segments to be unquestionably ZB rather than WZ. This maximal RTP density system, together with a half and a third of its density, i.e., one RTP every sixth and ninth layers of ZB, respectively, are shown in Fig. 3. For this reason, the maximally intermixed phase mixing system consists of two WZ layers every three layers of ZB. This system is shown in Fig. 3 (A), together with systems with double the WZ layers (four WZ layers every three layers of ZB) or double the ZB layers (two WZ layers every six layers of ZB), correspondingly.

To investigate how this anisotropy evolves in the defect systems, as the RTP or phase mixing density increases, the Born effective charge anisotropy is plotted in Fig. 4 as a function of the atoms fractional z-coordinate, since the z-axis lies along the [1 1 1]/[0 0 0 1]-direction. Positive anisotropies refer to higher Born effective charges along the [0 0 0 1]-direction as compared to the [1 0 1 0]-direction. Born effective charges describe the electrical polarisation induced by the displacement of individual atomic sublattices. The distribution of the Born effective charges in the material gives a quantitative assessment of the vibration resources, quantifying the coupling between macroscopic electric field and lattice deformation, which is directly linked to phonon scattering. Hence, positive or negative values of the Born effective charges describe the displacement of the charges of the neutral position.

The positive anisotropies belong to the Indium atoms, which also have positive Born effective charges, and the negative anisotropies belong to the Phosphorus atoms, which also have negative Born effective charges, i.e. large absolute anisotropies refer to larger Born effective charges along the [0 0 0 1]-direction.

Looking at the RTP systems, a large anisotropy is induced just around the RTP, which is then compensated for by the next few atoms having a lower than regular anisotropy. Interestingly, the anisotropy converges to a constant value of about 0.05 e in the ZB regions, where the anisotropy should be zero. Thus, the symmetry-breaking of even a single RTP must perturb the entire ZB segment, yielding a net anisotropy even in bulk Zincblende. This behaviour is not seen in the system with 1 RTP every 3 layers of ZB, which is likely because the RTPs are so close together that they interact with each other, forcing an even stronger compensation from the layers that do not belong to any RTP.

Looking at the phase mixing systems, the same convergence behaviour is seen in the Zincblende segments, with the anisotropy reaching a constant value of 0.05 e even in the smallest Zincblende segment. It is also seen that the Wurtzite segments reach the bulk Wurtzite anisotropy value even in the

smallest 2-layer segment, although only 1 of the layers reaches this value. Comparing the bulk WZ (or WZ segment) anisotropy value with the RTP induced anisotropy, it is clear that phase mixing induces larger Born charge anisotropies than RTPs.

Fig. 5 illustrates the phonon Density of States (DOS) calculated from the system phonon dispersions. It shows that all polytypic system DOSs look almost identical, yet with some clear differences from both ZB and WZ. Considering that the polytypic systems, and the phase mixing systems in particular, are systems mixed of the two phases, it would be expected that their DOSs would be somewhere in between those of WZ and ZB. Yet at various energies, particularly at 43 meV, the DOSs of the polytypic systems are all lower or higher than those of Zincblende and Wurtzite. It can be seen, though, that the DOSs of the polytypic systems more closely resemble WZ than ZB, considering that they miss the shoulder from 12 meV to 15 meV, have an additional side peak at 11 meV, have their peak at 20 meV moved to 18 meV and lack the high (0.9 meV−1) narrow peak at 37.4 meV.

One of the critical material parameters in a solid state is the complex dielectric function, which is related to electric susceptibility. The calculated Born effective charges and the dynamic matrixes are used to calculate the complex dielectric function in all the polytypic systems. The absorption coefficients can finally be calculated after calculating the dielectric function along both the K—and A-direction of the defect materials.

Fig. 6 shows the absorption coefficients of all polytypic systems. The absorption coefficient is calculated from the complex refractive index, which is simply the square root of the dielectric function: $n + ik = \sqrt{e_r}$ where n is the real refractive index, which is an important optical material property, and κ is the extinction coefficient, which is related to the optical absorption via the following relation: $a = 2\frac{w}{c}k$ where the c is the speed of light. We have calculated the absorption coefficients of all polytypic systems based on these equations.

From Fig. 6 it is clear that all polytypic systems resemble Zincblende, with a degree of resemblance depending on their Wurtzite content, as was to be expected since the absorption coefficients are calculated from the dielectric functions. The differences are harder to see in Fig. 6 than in the dielectric functions due to the scaling of the absorption coefficients with the electromagnetic frequency demanding a log scale to view them properly. In summary, all systems show a very similar profile to photo absorption. As expected, most of the absorption is in the ultraviolet part of the light spectrum. Hence, at least from the optical point of view, different types of RTP systems show almost identical behaviour.

IV. Conclusions

In conclusion, this work presents atomistic numerical simulations of InP bulk materials in the presence of RTP defects. Based on these simulations, we evaluated the underlying electronic structure and the photo-absorption of polytypic defect systems, i.e. systems that are a mix of Zincblende and Wurtzite. It was found that Wurtzite exhibits an anisotropy in its Born effective charges, in contrast to pristine Zincblende. It was also discovered that just one or two defects of Wurtzite in a Zincblende system also induce this anisotropy in the Zincblende section of the system, though to a lesser degree than in the Wurtzite section, thereby breaking its isotropy. In summary, our simulation results show that the number and orientation of the RTPs in InP have almost no impact on photon absorption.

References

[1] G. E. Stillman, V. M. Robbins, and N. Tabatabaie, "III-V compound semiconductor devices: Optical detectors," *IEEE Transactions on Electron Devices,* vol. 31, no. 11, pp. 1643-1655, 1984, doi: 10.1109/T-ED.1984.21765.

[2] B. Bahari, A. Ndao, F. Vallini, A. El Amili, Y. Fainman, and B. Kanté, "Nonreciprocal lasing in topological cavities of arbitrary geometries," *Science,* vol. 358, no. 6363, pp. 636-640, 2017/11/03 2017, doi: 10.1126/science.aao4551.

[3] G. E. Stillman, C. M. Wolfe, A. G. Foyt, and W. T. Lindley, "Schottky barrier InxGa1−xAs alloy avalanche photodiodes for 1.06 μm," *Applied Physics Letters,* vol. 24, no. 1, pp. 8-10, 1974, doi: 10.1063/1.1655004.

[4] N. Nakatsuka *et al.*, "Aptamer–field-effect transistors overcome Debye length limitations for small-molecule sensing," *Science,* vol. 362, no. 6412, pp. 319-324, 2018, doi: 10.1126/science.aao6750.

[5] N. Materise, M. C. Dartiailh, W. M. Strickland, J. Shabani, and E. Kapit, "Tunable capacitor for superconducting qubits using an InAs/InGaAs heterostructure," *Quantum Science and Technology,* vol. 8, no. 4, p. 045014, 2023/08/04 2023, doi: 10.1088/2058-9565/aceb18.

[6] C. D. Vedel, S. Smidstrup, and V. P. Georgiev, "First-principles investigation of polytypic defects in InP," *Scientific Reports,* vol. 12, no. 1, 2022, doi: 10.1038/s41598-022-24239-w.

[7] U. Krishnamachari *et al.*, "Defect-free InP nanowires grown in [001] direction on InP (001)," *Applied Physics Letters,* vol. 85, no. 11, pp. 2077-2079, 2004, doi: 10.1063/1.1784548.

[8] C. D. Vedel, T. Gunst, S. Smidstrup, and V. P. Georgiev, "Shockley-Read-Hall recombination and trap levels in $In_{0.53}Ga_{0.47}As$ as point defects from first principles," *Physical Review B,* vol. 108, no. 9, p. 094113, 09/26/ 2023, doi: 10.1103/PhysRevB.108.094113.

[9] Y. A. Bioud *et al.*, "Uprooting defects to enable high-performance III–V optoelectronic devices on silicon," *Nature Communications,* vol. 10, no. 1, p. 4322, 2019/09/20 2019, doi: 10.1038/s41467-019-12353-9.

[10] H. J. Joyce *et al.*, "Twin-Free Uniform Epitaxial GaAs Nanowires Grown by a Two-Temperature Process," *Nano Letters,* vol. 7, no. 4, pp. 921-926, 2007/04/01 2007, doi: 10.1021/nl062755v.

[11] H. Schmid *et al.*, "Template-assisted selective epitaxy of III–V nanoscale devices for co-planar heterogeneous integration with Si," *Applied Physics Letters,* vol. 106, no. 23, p. 233101, 2015/06/08 2015, doi: 10.1063/1.4921962.

[12] S. Smidstrup *et al.*, "QuantumATK: an integrated platform of electronic and atomic-scale modelling tools," *J Phys Condens Matter,* vol. 32, no. 1, p. 015901, Jan 1 2020, doi: 10.1088/1361-648X/ab4007.

[13] M. J. van Setten *et al.*, "The PseudoDojo: Training and grading a 85 element optimized norm-conserving pseudopotential table," *Computer Physics Communications,* vol. 226, pp. 39-54, 2018/05/01/ 2018, doi: https://doi.org/10.1016/j.cpc.2018.01.012.

[14] J. P. Perdew, K. Burke, and M. Ernzerhof, "Generalized Gradient Approximation Made Simple," *Physical Review Letters,* vol. 77, no. 18, pp. 3865-3868, 10/28/ 1996, doi: 10.1103/PhysRevLett.77.3865.

[15] P. Staudinger, S. Mauthe, K. E. Moselund, and H. Schmid, "Concurrent Zinc-Blende and Wurtzite Film Formation by Selection of Confined Growth Planes," *Nano Letters,* vol. 18, no. 12, pp. 7856-7862, 2018/12/12 2018, doi: 10.1021/acs.nanolett.8b03632.